Thermolysis of Fluorinated Single-Walled Carbon Nanotubes: Identification of Gaseous Decomposition Products by Matrix Isolation Infrared Spectroscopy

Holger F. Bettinger*

Lehrstuhl für Organische Chemie II, Ruhr-Universität Bochum, 44780 Bochum, Germany

Haiqing Peng

Center for Nanoscale Science and Technology, Rice University, Houston, Texas 77025

Received: August 5, 2005; In Final Form: September 26, 2005

The thermal decomposition of fluorinated single-walled carbon nanotubes (F−SWNTs), known to result in pristine SWNTs, has been investigated by freezing the gaseous products formed at temperatures between 50 and 500 °C under high vacuum in an argon matrix at 10−20 K and analyzing the trapped species by IR spectroscopy. The major products of F−SWNT decomposition are carbonyl fluoride (COF_2) below 300 °C and CF_4 above 300 °C. For comparison, graphite fluoride is stable thermally up to 300 °C under these conditions, and the major gas-phase species at temperatures below 500 °C are CF_4 and the CF_3 radical. F−SWNTs are thermally less stable than graphite fluoride, and etching of the nanotubes is observed at lower thermolysis temperatures.

Introduction

Fluorination provides an effective way of chemically modifying the properties of technologically relevant carbon materials.[1−4] A prominent example of this approach is fluorination of graphite, yielding graphite fluoride $(CF)_x$,[5−7] which is used as cathode material in today's lithium cells.[4] Other carbon materials have also been fluorinated and subsequently studied,[3,4] among them fullerenes[8,9] and nanotubes.[10−12] Single-walled carbon nanotubes (SWNTs), also called buckytubes, are of special importance as their small diameter results in unique and fascinating properties.[13,14] Fluorination of SWNTs has been reported in 1998,[15] and the available experimental and computational investigations have been reviewed.[16,17] It was found that C_2F is a limiting stoichiometry, as attempts to obtain even more highly fluorinated SWNTs by increasing reaction temperatures to 500 °C resulted in the destruction of the nanotube materials. Subsequent studies of the synthesized fluorinated SWNTs (F−SWNTs) have revealed some of their interesting (physico)chemical properties.[18−21] Among them are the increased solubility in organic solvents[18] and the fluorine substitution reaction with carbon nucleophiles.[19] An STM investigation discovered that the fluorine atoms are not distributed evenly on the nanotube surface, but rather, areas of a high degree of fluorination alternate with stripes essentially free of fluorine.[20] Computational investigations of F−SWNTs have been restricted to either small- to medium-sized carbon nanotube clusters[20,22−24] or relied on small unit cells in periodic computations.[25−28]

The recovery of pristine SWNTs from covalent derivatization (e.g., fluorine,[18] alkyl,[19] and carbene[29]) has prompted some investigations as to how strongly fluorine atoms are bound to the nanotube carbons.[27,30,31] It was found computationally that the mean C−F bond dissociation energies depend very strongly on the nanotube diameter.[27] The high-pressure CO (HiPco[32] process) produced material ($\phi \sim 1.0$ nm) should bind fluorine more strongly than the larger diameter laser oven produced SWNTs ($\phi \sim 1.35$ nm). The thermal recovery behavior of the latter has recently been carefully studied spectroscopically.[30,33] After annealing the fluorinated nanotubes (C/F ratios were 2 and 2.3) in inert gas atmospheres between 100 and 350 °C, UV−vis−near-IR and IR spectroscopic features of pristine SWNTs were observed.[30] XPS, Raman, and resistance measurements of the annealed samples indicate that most of the fluorine is lost at 200−300 °C, and at 400 °C the defluorination was found to be virtually complete, while the largest drop in resistance was at 150−200 °C.[33] The conduction mechanism, however, might be different than in pristine SWNTs, as Raman spectroscopy hints to a higher concentration of amorphous carbon.[33] While the tube bundles shortened, most of the F−SWNTs were recovered as SWNTs rather than being etched.[33] On the other hand, the high-temperature (up to 1000 °C) thermolysis of F−SWNTs (C/F ratio smaller than 5) in an argon atmosphere results in significantly shorter SWNTs (average < 50 nm) by etching (loss of CF_4).[31] A fluorination−defluorination protocol thus allows for controlled cutting of the carbon nanotubes.

To gain further insight into the properties of F−SWNTs and into the decomposition reactions they undergo at elevated temperatures, we here report an analysis of the volatile species evolved during the thermolysis of $(C_2F)_n$ F−SWNTs and comparison to the thermolysis behavior of fluorinated graphite, which has been studied extensively earlier.[4,34−37] Our study tries to answer the open questions concerning the defluorination mechanism and is thus complementary to the previous annealing studies by Zhao et al.,[30] Pehrsson et al.,[33] and Gu et al.,[31] which focused on the changes of the fluoronanotube samples[30,33] upon heating or very high applied temperatures.[31] To achieve this, the samples are heated under vacuum (10^{-5} mbar) in a matrix isolation apparatus and the volatile species evolving are frozen out in cryogenic argon matrixes (3−30 K) to allow their identification by means of IR spectroscopy. This approach is motivated by a number of benefits: (i) molecules frozen in cryogenic matrixes at sufficiently low temperatures are well separated from each other and immobile, and thus they do not

* Corresponding author.

10.1021/jp054370r CCC: $30.25
Published on Web 11/22/2005

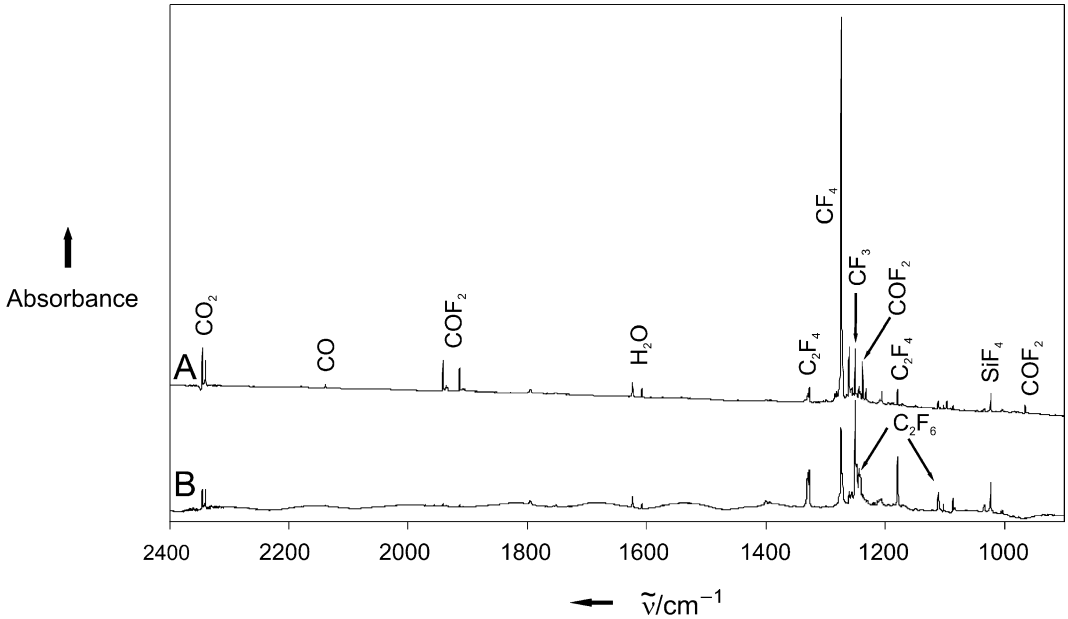

Figure 1. The IR spectra of the matrix-isolated species obtained from decomposition between 50 and 500 °C. (A) Fluorinated single-walled carbon nanotubes, $(C_2F)_n$. (B) Fluorinated graphite, $(CF_x)_n$ ($x \sim 1$).

react with each other; (ii) molecular rotations are frozen in cryogenic matrixes, resulting in very sharp absorption bands, which are essential for analysis of the complex fluorocarbon reaction product mixture; and (iii) the use of difference spectra allows the convenient monitoring of changes of the gas-phase composition at a given temperature, as indicated by the species trapped in cryogenic matrixes.

Experimental Section

The F−SWNT samples (prepared from HiPco[32] SWNTs) had C_2F stoichiometry and were synthesized as described previously by Gu et al.[31] Graphite fluoride $(CF_x)_n$ ($x \sim 1.0$) was purchased from Aldrich and was used without further purification. Matrix isolation experiments were performed by standard techniques with APD DE-204SL, APD DE-202, or Sumitomo Displex closed cycle helium cryostats. Samples (typically 0.6−1.0 mg) were placed in quartz glass tubes, which were heated resistively with a Ta (99.9%) wire. The temperature of the tube was measured with a thermocouple mounted on the exterior of the tube. The samples were heated in 50 °C steps from room temperature to the final temperature of 500 °C. At a given temperature all volatile species generated by thermolysis were co-deposited for 0.5 h with a large excess of argon (Messer Griesheim, 99.9999%) on top of a cold CsI window. The temperature of the CsI window increased during this procedure from 10 K to around 20 K at an oven temperature of 500 °C. The matrix temperatures could be kept under 5 K when we used the Sumitomo cryostat, but similar spectra were obtained. We therefore can exclude thermal reactions *after* the species have been matrix isolated. Matrix infrared spectra were recorded in the range 500−4000 cm^{-1} with a standard resolution of 0.5 cm^{-1} using either a Bruker Equinox 55 or a Bruker IFS-66 FTIR spectrometer equipped with a N_2(l)-cooled MCT detector.

The density functional computations using the B3LYP[38,39] hybrid functional in conjunction with Dunning's[40] correlation consistent basis set were conducted with the Gaussian 03[41] program.

Results

A. Species Identified in Ar Matrixes. General. Direct observation of atomic or molecular fluorine is certainly not possible by IR spectroscopy. It is well-known from the experiments of Jacox that co-deposition of F atoms and O_2 at 14 K results in the formation of FO_2 and O_2F_2, while matrix-isolated F_2 reacts with O_2 upon 650-nm irradiation at 14 K to O_2F_2.[42] We therefore performed trapping experiments with Ar:O_2 (99:1) mixtures, but we did not observe any of these O_2F_x species in our experiments. Consequently, we conclude that no free fluorine atoms or molecules are matrix isolated.

TABLE 1: Major Species and Their IR Signals Observed during Thermolysis of Fluorinated Single-Walled Carbon Nanotubes $(C_2F)_n$ and Fluorinated Graphite $(CF_x)_n$, $x \sim 1$

species	wavenumber/cm^{-1}	ref
HF	3963 R(0), 3955 (nonrotating), 3826 (dimer)	43
SiF_4	1023	44
COF_2	1941, 1914, 1238, 1232, 966, 769, 620, 584	45, 46
CF_4	1283, 1274, 1260, 1256, 631	47
CF_3	1250, 1087, 703	47
CF_2	1222, 1102	47
C_2F_4	1327, 1179	48
C_2F_6	1244, 1111	47
C_3F_6	1795, 1329, 1208, 1023	49, 50

Fluorotubes. We observe signals for CO_2, CO, and H_2O during the thermolyses of F−SWNTs. These species typically are observed in thermolysis experiments due to desorption from surfaces within the matrix apparatus at elevated temperatures and to small leaks in the vacuum system. However, control experiments and comparisons with graphite fluoride thermolyses (vide supra) suggest that the level of these species is slightly increased in fluoronanotube experiments. Integration of IR signals obtained at various thermolysis temperatures enabled, with help of literature data, the assignment of all major signals (Figure 1 and Table 1) to the following species: HF, SiF_4, COF_2, CF_4, CF_3, CF_2, C_2F_4, C_2F_6, and hexafluoropropene (C_3F_6).

Additional signals, which we could not assign, were observed at 1447 and 1119 cm^{-1} during thermolysis at $100 \leq T \leq 350$ °C and $100 \leq T \leq 150$ °C, respectively. Interestingly, bands at 1449 and 1119 cm^{-1} also remained unassigned in a 1992 study of the tetrafluoroethylene + O_2 reaction by Liu and Davis.[51] Furthermore, a few bands detected at higher thermolysis temperatures could also not be assigned unambiguously due to their very low intensities.

TABLE 2: Characteristic Experimental and Computed (B3LYP/cc-pVTZ) IR Absorptions, Symmetry Species, and Intensities Used To Derive the Relative Amount of Matrix Isolated Species

species	ν_{exp}/cm^{-1}	ω_{calc}/cm^{-1}	sym species	I_{calc}/ km mol^{-1}
HF	3963, 3955	4088	Σ	98
SiF_4	1023	1012	T_2	659
COF_2	769	780	B_1	35
CF_4	631	623	T_2	10
CF_3	703	697	A_1	12
CF_2	1102	1116	B_2	359
C_2F_4	1179	1187	B_{1u}	381
C_2F_6	1111	1111	A_{2u}	286
C_3F_6	1795	1829	A′	166

TABLE 3: Relative Abundances (in %) of Fluorine-Containing Species in the Matrixes Obtained after Successive Isolation of Gaseous Products between 50 and 500 °C

species	F-SWNT	graphite fluoride	species	F-SWNT	graphite fluoride
HF	19	0	CF_2	0	2
SiF_4	2	7	C_2F_4	3	18
COF_2	9	2	C_2F_6	1	6
CF_4	58	34	C_3F_6	4	6
CF_3	3	25			

Graphite Fluoride. Besides CO_2, CO, and H_2O, the following species were observed during thermolysis of graphite fluoride: CF_4, CF_3, C_2F_6, C_2F_4, SiF_4, and COF_2. Again, some very weak features observed at high temperatures could not be unambiguously assigned. A completely different composition of the matrix-isolated fluoride mixture compared to that seen for fluoronanotube thermolysis is observed (Figure 1).

B. Relative Composition of the Matrix-Isolated Gaseous Decomposition Products. To deduce the relative amounts of gas-phase species trapped in solid argon, we integrate the IR spectra depicted in Figure 1 at frequencies characteristic for the compounds identified. To allow comparison with earlier work on graphite fluoride decomposition, we determined the relative amounts of all gaseous fluorocarbons trapped after successive thermolyses in the 50−500 °C temperature range. As experimental IR extinction coefficients are not available for all compounds, we use intensities obtained from density functional computations at the B3LYP/cc-pVTZ level of theory (see Table 2).

Due to the overlap of the bands in the CF stretching region (1200−1300 cm^{-1}), the weak but well-separated deformation features were chosen for CF_4, CF_3, and COF_2 (the carbonyl stretching mode could not be used for this evaluation due to Fermi resonance, vide infra). While this approach does not allow us to derive the relative amounts of isolated species to high accuracy, it nonetheless should provide an order-of-magnitude estimate.

We find that the composition of the matrixes (depicted in Figure 1, Table 3) obtained after decomposition of fluoronanotubes and graphite fluoride between 50 and 500 °C differ significantly. The fluoronanotube thermolysis yields primarily HF (19%), COF_2 (9%), and CF_4 (58%). While CF_4 is also most prevalent in graphite fluoride decomposition under identical conditions, its yield is significantly reduced in favor of CF_3, C_2F_4, and C_2F_6. Ignoring the small amounts of CO, CO_2, and H_2O and adding the SiF_4 to CF_4, as done by Ruff and Bretschneider in their analysis of graphite fluoride decomposition,[5] average compositions of the gas mixtures of $CH_{0.21}O_{0.10}F_{3.57}$ and $CO_{0.01}F_{2.94}$ are obtained for fluoronanotube and graphite fluoride thermolyses, respectively.

C. Temperature Dependence of Gas-Phase Product Production. While CF_4 is overall most prevalent after 50−500 °C decomposition, it is, however, not the major product over the entire temperature range studied. As the products released from the tubes at various temperatures can possibly give a hint toward the major decomposition reactions, we briefly summarize the temperature dependence of product formation. This is achieved by a detailed analysis of the difference of IR spectra measured at successive temperatures, T and $T + 50$ °C (Figure 2). Any signal observed in a difference spectrum arises from a newly matrix isolated species at $T + 50$ °C. By comparing difference spectra, it is possible to learn if the evolution of a given species increased, decreased, or even stopped compared to the lower temperature condition.

Fluorotubes. The first fluorine-containing molecule observed is HF based on its absorptions at 3963 cm^{-1} (nonrotating) and 3955 cm^{-1} (rotating).[43] At higher temperatures, the $(HF)_2$ dimer is also observed (3826 cm^{-1}).[43] At $T = 200$ °C very weak signals due to COF_2 (1941 and 1914 cm^{-1}, arising from the Fermi resonance between ν_1 and $2\nu_2$) can be observed, while its ν_{as}(CF) band is detectable as a weak signal at 1238 cm^{-1}.[45,46,52] With increasing temperatures, the absorptions due to COF_2 increase significantly so that all other signals (966 and 769 cm^{-1}) assigned to COF_2 previously[45,46,52] are also detected in our experiments. The most intense signal of CF_4 is at 1274 cm^{-1}, which is observed first at $T = 250$ °C as a very weak feature.

The assignment of a very weak signal at 1023 cm^{-1} ($T = 150$ °C) is not straightforward, as SiF_4,[44] the FCO radical,[52] and hexafluoropropene (C_3F_6)[49,50] are reported to strongly absorb at this wavenumber. The FCO radical can be excluded, as its very strong signal at 1857 cm^{-1} is not observed even at temperatures when the 1023 cm^{-1} signal intensity significantly increased. Similarly, the 1795 cm^{-1} C═C stretching vibration of C_3F_6 has about the same intensity as the 1023 cm^{-1} absorption but is observable only at thermolysis temperatures $T \geq 300$ °C. Hence, we assign this band to SiF_4 at low thermolysis temperatures, but note that some of the intensity of this signal arises from C_3F_6 at higher temperatures. In the 250−300 °C temperature range, a number of other fluorocarbon molecules are also observed for the first time: C_2F_4 (1179 cm^{-1}),[47,48] CF_3 (1250 cm^{-1}), C_2F_6, and C_3F_6 (1795, 1208). The signals due to these species increase in intensity with increasing temperatures, but not as dramatically as those of CF_4.

At temperatures $T \leq 300$ °C, the HF and COF_2 molecules are the major gas-phase products of fluoronanotube thermolysis. In the 50−300 °C temperature range already about 65% of the total (50−500 °C) HF is obtained, in contrast to about 10% of the total COF_2 production. While the COF_2 formation is still ongoing at higher temperatures, it is outrun by CF_4 production: CF_4 is the by far the major product of fluoronanotube thermolysis already at 400 °C (Figure 3).

Graphite Fluoride. No volatile fluorine-containing gas-phase species are observed at $T \leq 300$ °C, while at $T = 350$ °C extremely weak signals due to CF_4 (1274 cm^{-1}), CF_3 (1250 cm^{-1}), C_2F_4 (1179 cm^{-1}), and SiF_4 (1023 cm^{-1}) are discernible. At 400 °C the intensity of these signals increases, with the 1023 cm^{-1} SiF_4 band being the most intense. But this is no longer the case at 450 °C, when the signals due to CF_4 (1274 cm^{-1}) and CF_3 (1250 cm^{-1}) are more intense than those due to SiF_4. In addition, CF_2 (1102 cm^{-1}) can now be detected. The bands of COF_2 are only visible at $T = 500$ °C and even then remain weak compared to the strong signals due to CF_4, CF_3, and C_2F_4.

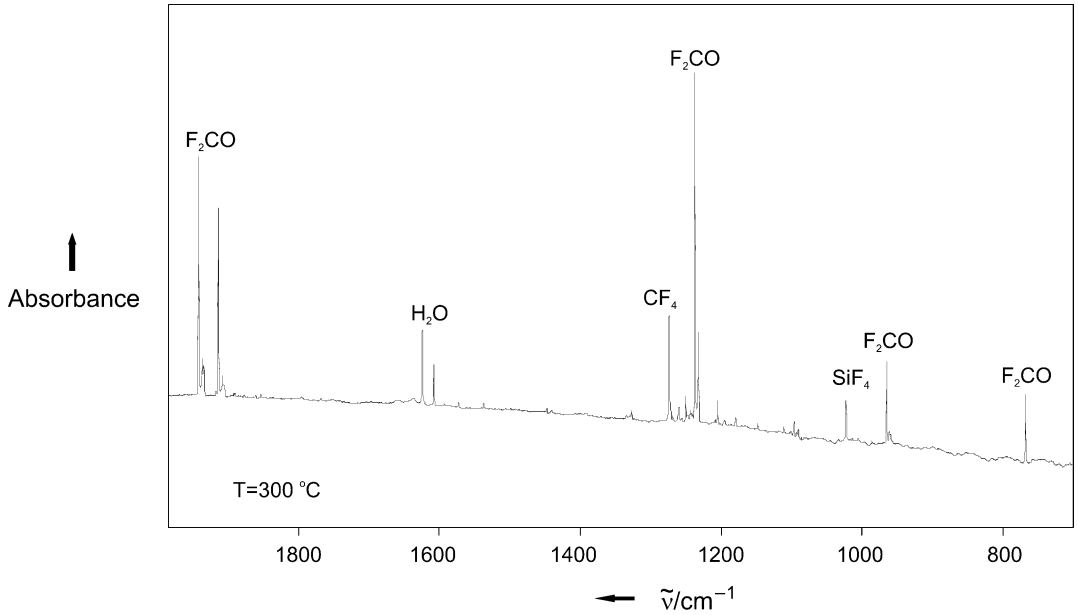

Figure 2. Difference spectrum obtained from the thermolysis at 300 and 250 °C of fluorinated single-walled carbon nanotube sample $(C_2F)_n$.

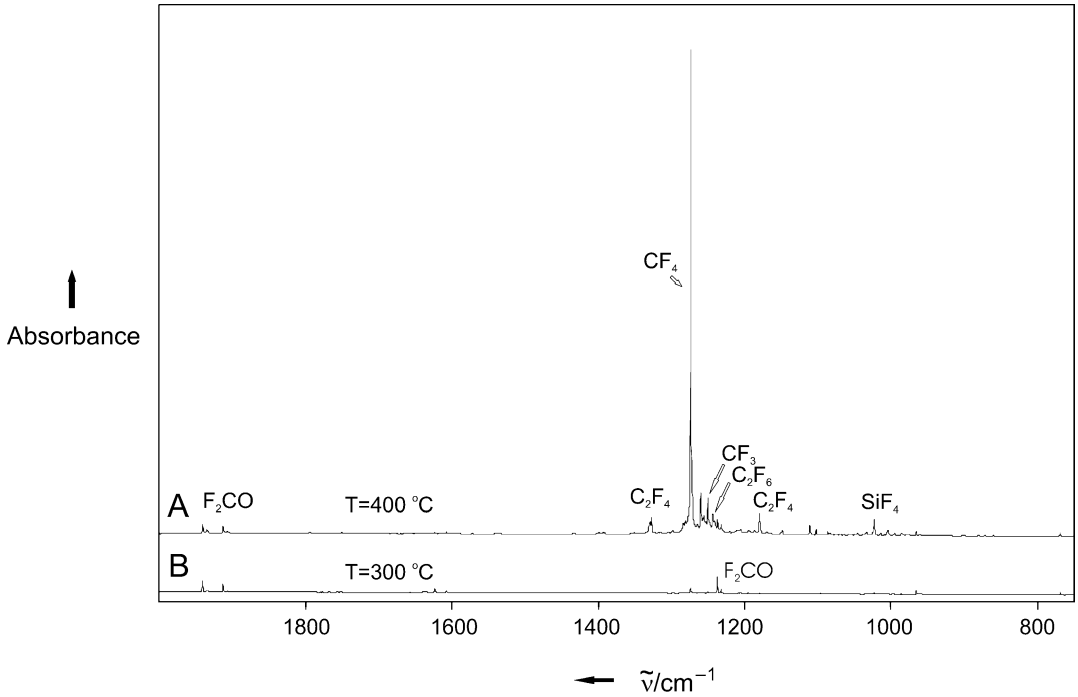

Figure 3. Difference spectra obtained at the thermolysis temperatures 400−350 °C (labeled as $T = 400$ °C) and 300−250 °C (labeled as $T = 300$ °C) of fluorinated single-walled carbon nanotube sample $(C_2F)_n$. Note that the $T = 300$ °C difference spectrum is already given in Figure 2 but reproduced here to stress the different scales of the ordinate axes.

Discussion

Before discussing a possible mechanistic scenario for F−SWNT decomposition and comparing with decomposition of graphite fluorides $(CF)_n$ and $(C_2F)_n$, we address the formation of the two products, carbonyl fluoride (COF_2) and silicon tetrafluoride (SiF_4), with elements not included in the fluorocarbons.

A. Origin of the Oxygen-Containing Products. Formation of an oxygen-containing product, carbonyl fluoride, as a major product at $T \leq 300$ °C from the thermolysis of a carbon−fluorine material is clearly unexpected. As the fluorinated graphite did not yield any COF_2 under identical conditions, its formation in the F−SWNT thermolysis indicates that the F−SWNT samples contain oxygen to some minor amount. Indeed, Marcoux et al. observed in an XPS investigation of fluorinated laser-oven SWNT samples that the C 1s massif includes six components, among them are C−OH, carbonyl, and carboxyl functionalities.[21] The composition of gas-phase species isolated in the argon matrix, $CH_{0.21}F_{3.57}O_{0.10}$, corresponds to an elemental oxygen percentage of about 2%. A similar percentage, 2.8%, was deduced by Marcoux et al. for their highly fluorinated laser-oven nanotube sample of $C_{1.9}F$ stoichiometry.[21] This group has ascribed the oxygen contamination to the oxidative treatment during the cleanup of the tubes. Also absorption or reaction of oxygen-containing molecules during handling of the F−SWNTs cannot be excluded, especially in view of the large surface area of the F−SWNT samples (∼500 m^2/g). Fluorinated larger fullerenes are well-known to react

readily with atmospheric moisture.[8,53] Taylor, for example, isolated from the fluorination of C_{70} with MnF_3 a number of $C_{70}F_xO_y$ and $C_{70}F_xO_2H$ products, identified as epoxides and hydroxides.[53] We therefore conclude that chemically bound oxygen is released from the tubes in the form of COF_2, CO_2, and CO at lower temperatures. A similar suggestion has been made by Gu et al.,[31] who observed carbonyl fluoride during the high-temperature decomposition of $(C_nF)_x$ ($n > 5$) F−SWNT samples in argon at 1 atm pressure.

B. Origin of HF and SiF_4. The formation of HF and SiF_4 is observed already at a low thermolysis temperatures, albeit in a very small amount. HF was used as a catalyst in the F−SWNT synthesis and might be physisorbed to the nanotubes. This physisorption might explain why a large amount (in excess of 60%) of the HF formed overall in the 50−500 °C temperature range is already isolated at $T \leq 300$ °C. It could also be a product of the reaction of fluorine containing intermediates with trace amounts of water. While the exact mechanisms accounting for SiF_4 formation are unclear, we note that SiF_4 formation has previously been observed in graphite fluoride thermolyses if conducted in quartz glass,[5,36,37] and its fluorine content added to that of CF_4 in the quantitative analysis of Ruff and Bretschneider.[5] Interestingly, formation of SiF_4 was also observed during the hydrolysis of fluorinated [60]fullerene in an NMR tube.[54] Decomposition of the stable fluorocarbons (CF_4, C_2F_6, and C_2F_4) should not be a source of SiF_4 in our experiments. It is known from the experiments of Atkinson and Atkinson that C_2F_4 does not react with Pyrex glass at temperatures below 700 °C.[55] Likewise, CF_4 is a very stable compound thermally, and control experiments show that it does not react with our oven material at the temperatures used in our experiments.

C. Comparison with Thermal Decomposition of Graphite Fluorides $(CF)_n$ and $(C_2F)_n$ and Speculations on the Decomposition Mechanism. Thermal decomposition of graphite fluorides has been well-studied,[4,34−37] and a comparison with that of fluorinated nanotubes is instructive. Ruff et al. found in 1934 that the gradual high-vacuum decomposition of $(CF)_n$ prepared from graphite starts very slowly around 300 °C and is most violent at 500−600 °C.[5] The gas mixture was dominated by C_2F_6, but also C_5F_{12} (or similar fluorides), CF_4, and C_2F_4 (besides SiF_4, CO, and CO_2) were obtained. The solid residue was found to be pure graphite, while the average composition of the gases was $CF_{2.81}$.[5] In contrast, explosive decomposition was reported by Ruff et al. to result in an average $CF_{3.7}$ gas-phase compound composition and soot as solid residue,[5] indicating that the decomposition process has a significant temperature dependence. Kamarchik and Margrave studied the thermal decomposition of $(CF)_n$ by means of isothermal-gravimetric analyses as well as by matrix isolation of gaseous products, similar to the approach adopted in the present work.[34] These authors reported the observation of a wide range of products, with CF_4, C_2F_4, and C_2F_6 being the most prominent, and also provided a kinetic analysis of the thermal decomposition.[34] The apparent average F/C ratio of 2.0 for all the gas-phase species led Kamarchik and Margrave to suggest that decomposition is occurring at the edges of $(CF)_n$ crystallites under C_2F_4 evolution.[34] Watanabe et al. studied the thermal $(CF)_n$ decomposition extensively.[4,36,37] They found C_2F_6 to be most prevalent (CF_4, C_2F_4, C_3F_8, and C_3F_6 were also detected) after trapping gaseous products of vacuum decomposition (fixed temperatures between 567 °C and 663 °C) in a cold trap.[4,37] On the basis of detailed analysis of reaction kinetics, gaseous products, and solid residues, Watanabe et al. suggested a mechanism that involves decomposition of every other layer of $(CF)_x$ under CF_2 formation[37] and stressed the importance of stress at grain boundaries for the formation of nucleation sites.[36]

Our observations of CF_4, C_2F_4, and C_2F_6 are in agreement with these previous investigations. Interestingly, we also detect large amounts of the CF_3 radical. Under Watanabe's[36,37] and Ruff's[5] experimental conditions, condensation of gaseous species in a cold trap, observation of this unstable radical is not possible due to further reactions, e.g., dimerization to C_2F_6 (the most prevalent species in Watanabe's[36,37] experiment). The average gas-phase composition of $CF_{2.9}$ obtained in our experiment is in agreement with the average $CF_{2.8}$ composition of gas-phase products observed by Ruff et al.[5]

We now turn our attention to the fluorocarbons of $(C_2F)_n$ composition, stage 2 covalent graphite fluoride, $(C_2F)_n$, and fluoronanotubes. Watanabe et al.[4] found that the thermolysis of $(C_2F)_n$ results primarily in the formation of CF_4, despite its lower fluorine content. Similar types of analyses as for $(CF)_n$ led Watanabe et al. to conclude that the decomposition of $(C_2F)_n$ starts with the rupture of C−F bonds.[4] The structure of stage 2 graphite fluoride $(C_2F)_n$, C−C bonds interconnecting the six membered rings (chair conformation) of two neighboring sheets with fluorine placed on the top side of one carbon sheet and the bottom side of the other sheet, precludes the decomposition mechanism suggested for $(CF)_n$. It is remarkable that the thermal decomposition of F−SWNTs, which ideally also have only one side of their surface fluorinated, similarly results primarily in CF_4.

Carbon tetrafluoride (CF_4) is the thermodynamically most stable species compared to the CF_3 radical and CF_2 carbene. These reactive intermediates, in particular CF_2, are central to the decomposition process, as the two and three carbon atoms containing molecules C_2F_6, C_2F_4, and C_3F_6 can be regarded as their dimerization and trimerization products, while CF_4 can be considered to result from them by successive fluorine atom uptake.

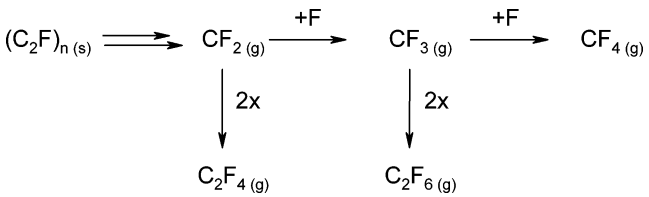

The amount of CF_4 formed during the decomposition compared to other fluorocarbons then is an indicator of the apparent barrier for the process of releasing fluorine from the solid fluorocarbon. It appears that fluoronanotubes are less stable thermally than graphite fluoride at a given temperature and that thus the formation of the thermodynamically favored gas-phase species is observed at lower temperatures. However, the influence of remaining catalyst particles is unknown.

Our experiments do not allow deducing any information on the atomic mechanisms of the decomposition of the solid material. However, in both fluoronanotube and graphite fluoride thermolyses, the formation of SiF_4 is observed at the onset of decomposition, and it is thus tempting to assume a similar initial process, rupture of C−F bonds. Once C−F bonds are broken, fluorine atoms or molecules would then be able to react with the surface of the quartz glass oven to result in SiF_4. This is observed, however, at rather different temperatures for fluoronanotubes (100−150 °C) and graphite fluoride (350−400 °C). With increasing temperature, the concentration of reactive fluorine increases, and accordingly, more SiF_4 is formed. The

onset of SiF_4 formation in fluoronanotube thermolysis at rather low temperatures might however also be due to the presence of HF, which with traces of water can etch the quartz glass surface. In addition, some C−C bonds can break, presumably those close to defects in the nanotube sidewall (where CF_2 groups can reside) or at grain boundaries in graphite fluoride. Hence, etching of the carbon backbone sets in, and CF_2, a thermodynamically rather stable singlet carbene, should play a prominent role as a gas-phase species in the decomposition. The very weak signal at 1102 cm^{-1} observed at low temperatures during F−SWNT thermolysis could indicate that CF_2 might be able to escape the reaction zone, but as no other signals due to CF_2 can be detected under these conditions, this is not clear beyond doubt. Dimerization of CF_2 yields C_2F_4, which is observed in fluoronanotube thermolysis at temperatures below the onset of CF_3 and CF_4 formation. Also signals due to CF_4 appear before those of the CF_3 radical in fluoronanotube thermolysis. An explanation of CF_4 formation at rather low temperatures might be the disproportionation reaction:

$$2CF_2 = C(s) + CF_4$$

Operation of this reaction might explain the increased amount of amorphous carbon in the SWNT samples reported by Pehrsson et al.[33] and the black carbon film on the glass surface downstream from the F−SWNT sample in our experiments. This film is not observed in $(CF)_n$ thermolysis; here, CF_4, CF_3, and C_2F_4 formation sets in at the same temperature, $T = 350$ °C.

Rearrangements of the fluorine atoms on the curved or planar π surfaces should have energy requirements lower than C−F bond breaking, and thus this mechanism can provide a flux of fluorine to reactive sites. As the C−F bonds in fluoronanotubes are generally weaker than in graphite fluoride,[27] the thermodynamically most stable product, CF_4, is obtained already at lower temperatures.

Conclusions

From the above analysis of the products and their evolution during thermolysis we conclude the following:

(1) In agreement with previous XPS[21,33] and TGA[31] investigations, we find that the fluoronanotubes have bound significant amounts of oxygen, which is driven off the tubes in the form of COF_2, CO_2, and CO at rather low temperatures. It is therefore highly desirable to study fluoronanotubes that have been handled under inert atmospheres, in future experiments.

(2) Even though the processes of fluoronanotube and graphite fluoride thermolyses are similar overall, the fluoronanotubes are thermally less stable than graphite fluoride. The fluorinated HiPco tubes (H-FSWNTs) we investigated here are thermally more stable than the laser-oven fluoronanotubes (L-FSWNTs) investigated by Zhao et al.[30] and Pehrsson et al.[33] The increasing thermal stability L-FSWNT < H-FSWNT < $(CF)_n$ is in agreement with a previous comparative electrochemical investigation[56] and with computational results.[27] However, the oxygen content and the CF bond breaking at unexpectedly low temperatures suggest that the experimental material has a significant amount of defects. Possibly the large decrease in resistance observed after low-temperature annealing (150−200 °C) might be associated with desorption of weakly bound ("misplaced") fluorine and rearrangements of the fluorine atoms on the nanotube surface.

(3) Etching of the nanotubes during thermolysis is not limited to very high temperatures,[31] but it is also observed at lower temperatures. As the decomposition starts with SiF_4 formation and thus likely with CF bond breaking, a very careful thermal treatment at lower temperatures could possibly limit etching to a minimum.

Acknowledgment. In memoriam of Professor John L. Margrave. H.F.B. is grateful to Prof. W. Sander, who kindly provided access to the matrix isolation equipment, and to the Fonds der Chemischen Industrie, for financial support through a Liebig Fellowship.

References and Notes

(1) Touhara, H.; Okino, F. *Carbon* **2000**, *38*, 241.
(2) Touhara, H.; Inahara, J.; Mizuno, T.; Yokoyama, Y.; Okanao, S.; Yanagiuch, K.; Mukopadhyay, I.; Kawasaki, S.; Okino, F.; Shirai, H.; Xu, W. H.; Kyotani, T.; Tomita, A. *J. Fluorine Chem.* **2002**, *114*, 181.
(3) *Fluorine−Carbon and Fluoride-Carbon Materials*; Nakajima, T., Ed.; Marcel Dekker: New York, 1995.
(4) Watanabe, N.; Nakajima, T.; Touhara, H. *Graphite Fluorides*; Elsevier: Amsterdam, 1988.
(5) Ruff, O.; Bertschneider, O.; Evert, F. *Z. Anorg. Allg. Chem.* **1934**, *217*, 1.
(6) Rüdorff, W.; Rüdorff, G. *Z. Anorg. Chem.* **1947**, *253*, 281.
(7) Rüdorff, W.; Rüdorff, G. *Chem. Ber.* **1947**, *80*, 413.
(8) Taylor, R. *Chem. Eur. J.* **2001**, *7*, 4075.
(9) Neretin, I. S.; Lyssenko, K. A.; Antipin, M. Y.; Slovokhotov, Y. L. *Russ. Chem. Bull.* **2002**, *51*, 754.
(10) Nakajima, T.; Kasamatsu, S.; Matsuo, Y. *Eur. J. Solid State Inorg. Chem.* **1996**, *33*, 831.
(11) Hamwi, A.; Alvergnat, H.; Bonnamy, S.; Beguin, F. *Carbon* **1997**, *35*, 723.
(12) Okotrub, A. V.; Yudanov, N. F.; Chuvilin, A. L.; Asanov, I. P.; Shubin, Y. V.; Bulusheva, L. G.; Gusel'nikov, A. V.; Fyodorov, I. S. *Chem. Phys. Lett.* **2000**, *322*, 231.
(13) Dresselhaus, M. S.; Dresselhaus, G.; Eklund, P. C. *Science of Fullerenes and Carbon Nanotubes*; Academic Press: New York, 1996.
(14) *Carbon Nanotubes: Synthesis, Structure, Properties, and Applications*; Dresselhaus, M. S., Dresselhaus, G., Avouris, P., Eds.; Springer: Berlin, 2001.
(15) Mickelson, E. T.; Huffman, C. B.; Rinzler, A. G.; Smalley, R. E.; Hauge, R. H.; Margrave, J. L. *Chem. Phys. Lett.* **1998**, *296*, 188.
(16) Khabashesku, V. N.; Billups, W. E.; Margrave, J. L. *Acc. Chem. Res.* **2002**, *35*, 1087.
(17) Bettinger, H. F. *Chem. Phys. Chem.* **2003**, *4*, 1283.
(18) Mickelson, E. T.; Chiang, I. W.; Zimmerman, J. L.; Boul, P. J.; Lozano, J.; Liu, J.; Smalley, R. E.; Hauge, R. H.; Margrave, J. L. *J. Phys. Chem. B* **1999**, *103*, 4318.
(19) Boul, P. J.; Liu, J.; Mickelson, E. T.; Huffman, C. B.; Ericson, L. M.; Chiang, I. W.; Smith, K. A.; Colbert, D. T.; Hauge, R. H.; Margrave, J. L.; Smalley, R. E. *Chem. Phys. Lett.* **1999**, *310*, 367.
(20) Kelly, K. F.; Chiang, I. W.; Mickelson, E. T.; Hauge, R. H.; Margrave, J. L.; Wang, X.; Scuseria, G. E.; Radloff, C.; Halas, N. J. *Chem. Phys. Lett.* **1999**, *313*, 445.
(21) Marcoux, P. R.; Schreiber, J.; Batail, P.; Lefrant, S.; Renouard, J.; Jacob, G.; Albertini, D.; Mevellec, J.-Y. *Phys. Chem. Chem. Phys.* **2002**, *4*, 2278.
(22) Bauschlicher, C. W. *Chem. Phys. Lett.* **2000**, *322*, 237.
(23) Breslavskaya, N. N.; D'yachov, P. N. *Russ. J. Inorg. Chem.* **2000**, *45*, 1685.
(24) Jaffe, R. L. *J. Phys. Chem. B* **2003**, *107*, 10378.
(25) Seifert, G.; Köhler, T.; Frauenheim, T. *Appl. Phys. Lett.* **2000**, *77*, 1313.
(26) Kudin, K. N.; Bettinger, H. F.; Scuseria, G. E. *Phys. Rev. B* **2001**, 045413.
(27) Bettinger, H. F.; Kudin, K. N.; Scuseria, G. E. *J. Am. Chem. Soc.* **2001**, *123*, 12849.
(28) Park, K. A.; Choi, Y. S.; Lee, Y. H.; Kim, C. *Phys. Rev. B* **2003**, *68*, 045429/1.
(29) Holzinger, M.; Vostrowsky, O.; Hirsch, A.; Hennrich, F.; Kappes, M.; Weiss, R.; Jellen, F. *Angew. Chem.* **2001**, *113*, 4132.
(30) Zhao, W.; Song, C.; Zheng, B.; Liu, J.; Viswanathan, T. *J. Phys. Chem. B* **2002**, *106*, 293.
(31) Gu, Z.; Peng, H.; Hauge, R.; Smalley, R. E.; Margrave, J. L. *Nano Lett.* **2002**, *2*, 1009.
(32) Nikolaev, P.; Bronikowski, M. J.; Bradley, R. K.; Rohmund, F.; Colbert, D. T.; Smith, K. A.; Smalley, R. E. *Chem. Phys. Lett.* **1999**, *313*, 91.
(33) Pehrsson, P. E.; Zhao, W.; Baldwin, J. W.; Song, C.; Liu, J.; Kooi, S.; Zheng, B. *J. Phys. Chem. B* **2003**, *107*, 5690.
(34) Kamarchik, P.; Margrave, J. L. *J. Therm. Anal.* **1977**, *11*, 259.

(35) Watanabe, N.; Kawamura, T.; Koyama, S. *Bull. Chem. Soc. Jpn.* **1980**, *53*, 3100.
(36) Watanabe, N.; Koyama, S. *Bull. Chem. Soc. Jpn.* **1980**, *53*, 3093.
(37) Watanabe, N.; Koyama, S.; Imoto, H. *Bull. Chem. Soc. Jpn.* **1980**, *53*, 2731.
(38) Becke, A. D. *J. Chem. Phys.* **1993**, *98*, 5648.
(39) Lee, C.; Yang, W.; Parr, R. G. *Phys. Rev. B* **1988**, *37*, 785.
(40) Dunning, T. H. *J. Chem. Phys.* **1989**, *90*, 1007.
(41) Frisch, M. J.; Trucks, G. W.; Schlegel, H. B.; Scuseria, G. E.; Robb, M. A.; Cheeseman, J. R.; Montgomery, J. A., Jr.; Vreven, T.; Kudin, K. N.; Burant, J. C.; Millam, J. M.; Iyengar, S. S.; Tomasi, J.; Barone, V.; Mennucci, B.; Cossi, M.; Scalmani, G.; Rega, N.; Petersson, G. A.; Nakatsuji, H.; Hada, M.; Ehara, M.; Toyota, K.; Fukuda, R.; Hasegawa, J.; Ishida, M.; Nakajima, T.; Honda, Y.; Kitao, O.; Nakai, H.; Klene, M.; Li, X.; Knox, J. E.; Hratchian, H. P.; Cross, J. B.; Adamo, C.; Jaramillo, J.; Gomperts, R.; Stratmann, R. E.; Yazyev, O.; Austin, A. J.; Cammi, R.; Pomelli, C.; Ochterski, J. W.; Ayala, P. Y.; Morokuma, K.; Voth, G. A.; Salvador, P.; Dannenberg, J. J.; Zakrzewski, V. G.; Dapprich, S.; Daniels, A. D.; Strain, M. C.; Farkas, O.; Malick, D. K.; Rabuck, A. D.; Raghavachari, K.; Foresman, J. B.; Ortiz, J. V.; Cui, Q.; Baboul, A. G.; Clifford, S.; Cioslowski, J.; Stefanov, B. B.; Liu, G.; Liashenko, A.; Piskorz, P.; Komaromi, I.; Martin, R. L.; Fox, D. J.; Keith, T.; Al-Laham, M. A.; Peng, C. Y.; Nanayakkara, A.; Challacombe, M.; Gill, P. M. W.; Johnson, B.; Chen, W.; Wong, M. W.; Gonzalez, C.; Pople, J. A. *Gaussian 03*, Revision B.4; Gaussian, Inc.: Pittsburgh, PA, 2003.
(42) Jacox, M. E. *J. Mol. Spectrosc.* **1980**, *84*, 74.
(43) Hunt, R. D.; Andrews, L. *J. Chem. Phys.* **1985**, *82*, 4442.
(44) Bassler, J. M.; Timms, P. L.; Margrave, J. L. *Inorg. Chem.* **1966**, *5*, 729.
(45) Bouteiller, Y.; Abdelaoui, O.; Schriver, A.; Schriver-Mazzuoli, L. *J. Chem. Phys.* **1995**, *102*, 1731.
(46) Mallinson, P. D.; McKean, D. C.; Holloway, J. H.; Oxton, I. A. *Spectrochim. Acta A* **1975**, *31*, 143.
(47) Milligan, D. E.; Jacox, M. E. *J. Chem. Phys.* **1968**, *48*, 2265.
(48) Ozin, G. A.; Power, W. J. *Inorg. Chem.* **1977**, *16*, 2864.
(49) Jacox, M. E. *J. Phys. Chem.* **1984**, *88*, 445.
(50) Kelsall, B. J.; Andrews, L. *J. Phys. Chem.* **1981**, *85*, 1288.
(51) Liu, L.; Davis, S. R. *J. Phys. Chem.* **1992**, *96*, 9719.
(52) Jacox, M. E. *J. Mol. Spectrosc.* **1980**, *80*, 257.
(53) Taylor, R.; Abdul-Sada, A. K.; Boltalina, O. V.; Street, J. M. *J. Chem. Soc., Perkin Trans. 2* **2000**, 1013.
(54) Taylor, R.; Holloway, J. H.; Hope, E. G.; Avent, A. G.; Langley, G. J.; Dennis, T. J.; Hare, J. P.; Kroto, H. W.; Walton, D. R. M. *J. Chem. Soc., Chem. Commun.* **1992**, 665.
(55) Atkinson, B.; Atkinson, V. A. *J. Chem. Soc.* **1957**, 2086.
(56) Peng, H.; Gu, Z.; Yang, J.; Zimmerman, J. L.; Willis, P. A.; Bronikowski, M. J.; Smalley, R. E.; Hauge, R.; Margrave, J. L. *Nano Lett.* **2001**, *1*, 625.